J Neurooncol (2016) 126:279–288
DOI 10.1007/s11060-015-1960-5

CLINICAL STUDY

Advanced MRI may complement histological diagnosis of lower grade gliomas and help in predicting survival

Valeria Cuccarini[1] · A. Erbetta[1] · M. Farinotti[2] · L. Cuppini[3] · F. Ghielmetti[1] · B. Pollo[4] · F. Di Meco[5] · M. Grisoli[1] · G. Filippini[2] · G. Finocchiaro[3] · M. G. Bruzzone[1] · M. Eoli[3]

Received: 25 February 2015 / Accepted: 8 October 2015 / Published online: 14 October 2015

Abstract MRI grading of grade II and III gliomas may have an important impact on treatment decisions. Occasionally, both conventional MRI (cMRI) and histology fail to clearly establish the tumour grade. Three cMRI features (no necrosis; no relevant oedema; absent or faint contrast enhancement) previously validated in 196 patients with supratentorial gliomas directed our selection of 68 suspected low-grade gliomas (LGG) that were also investigated by advanced MRI (aMRI), including perfusion weighted imaging (PWI), diffusion weighted imaging (DWI) and spectroscopy. All the gliomas had histopathological diagnoses. Sensitivity and specificity of cMRI preoperative diagnosis were 78.5 and 38.5 %, respectively, and 85.7 and 53.8 % when aMRI was included, respectively. ROC analysis showed that cut-off values of 1.29 for maximum rCBV, 1.69 for minimum rADC, 2.1 for rCho/Cr ratio could differentiate between LGG and HGG with a sensitivity of 61.5, 53.8, and 53.8 % and a specificity of 54.7, 43 and 64.3 %, respectively. A significantly longer OS was observed in patients with a maximum rCBV <1.46 and minimum rADC >1.69 (80 vs 55 months, $p = 0.01$; 80 vs 51 months, $p = 0.002$, respectively). This result was also confirmed when cases were stratified according to pathology (LGG vs HGG). The ability of aMRI to differentiate between LGG and HGG and to predict survival improved as the number of aMRI techniques considered increased. In a selected population of suspected LGG, classification by cMRI underestimated the actual fraction of HGG. aMRI slightly increased the diagnostic accuracy compared to histopathology. However, DWI and PWI were prognostic markers independent of histological grade.

Keywords Conventional MRI · Diffusion-weighted images · Lower-grade glioma · Overall survival · Perfusion-weighted images · Spectroscopy

Background

Low-grade gliomas (LGG) represent 30 % of all gliomas and include tumors with astrocytic and/or oligodendroglial features [1]. Natural evolution is towards malignancy but survival rate varies from less than 2 years to more than 10 years. Clinical approaches range from "wait and see" to early diagnosis through biopsy or surgical resection [2]. Subsequent treatments must be carefully evaluated given the possibility of long-term adverse effects. For these reasons, non-invasive, pre-surgical diagnosis and grading are fundamental in the decision-making process and clinical management.

Although conventional Magnetic Resonance Imaging (cMRI) with contrast agents is an established and useful

Electronic supplementary material The online version of this article (doi:10.1007/s11060-015-1960-5) contains supplementary material, which is available to authorized users.

✉ Valeria Cuccarini
valeria.cuccarini@istituto-besta.it

[1] Unit of Neuro-Radiology, Fondazione IRCCS Istituto Neurologico Carlo Besta, Via Celoria 11, 20133 Milan, Italy

[2] Unit of Neuro-Epidemiology, Fondazione IRCCS Istituto Neurologico Carlo Besta, Via Celoria 11, 20133 Milan, Italy

[3] Unit of Molecular Neuro-Oncology, Fondazione IRCCS Istituto Neurologico Carlo Besta, Via Celoria 11, 20133 Milan, Italy

[4] Unit of Neuro-Pathology, Fondazione IRCCS Istituto Neurologico Carlo Besta, Via Celoria 11, 20133 Milan, Italy

[5] Unit of Neuro-Surgery I, Fondazione IRCCS Istituto Neurologico Carlo Besta, Via Celoria 11, 20133 Milan, Italy

tool in the characterization of cerebral tumours, its sensitivity for classification and grading of gliomas ranges 55–83 % [3, 4]. High-grade glioma (HGG) may be misdiagnosed as LGG by cMRI in the absence of oedema, contrast enhancement (CE), or necrosis. In contrast, CE has been reported in up to 40 % of LGG [5]. Furthermore, cMRI doesn't provide information about blood volume, angiogenesis, micronecrosis, cellularity, which are important features to define tumour grade [4].

Advanced MRI (aMRI), such as diffusion- and perfusion-weighted imaging (DWI and PWI, respectively) and magnetic resonance spectroscopy (MRS), have been widely used in pre-surgical assessment and follow-up of gliomas [6]. Unlike CE, increased perfusion is generally independent of blood–brain-barrier integrity and defines tumour neoangiogenesis [7]. On DWI, the apparent diffusion coefficient (ADC) inversely correlates to cellularity and reflects tumour infiltration before changes are visible on cMRI [8]. MRS provides information about the metabolites choline (Cho), *N*-acetyl aspartate (NAA), and lipids/lactate, useful for tumour grading [4].

Several studies focused on the usefulness of aMRI in gliomas [3, 4, 8–20], suggesting a relationship of cut-off values to histopathology [4, 21–26] and, more recently, to survival [10, 20, 25, 27–35].

Even though neuropathology is still considered the gold standard in glioma diagnosis, its limitations due to tumour heterogeneity and insufficiently representative specimens [27] are acknowledged.

Aims of the present study were to assess the possible pre-operative diagnostic advantage of associating aMRI (DWI, PWI, MRS) to cMRI in a group of selected patients suspected to have LGG based on cMRI and to investigate whether aMRI can be useful in the prediction of outcome (overall survival [OS] and progression-free survival [PFS]).

Methods

Patients

This prospective observational study of radiological diagnosis of gliomas was performed at the Neurological Institute Besta, Milan, Italy. Institution Ethics Committee was regularly informed about the study, and informed consent was obtained from all participants. Between 2006 and 2009, adult patients with suspected supratentorial glioma according to pre-surgical cMRI were considered for inclusion. Patients scheduled for biopsy, who had already undergone biopsy/surgery, or treated with chemo- or radiotherapy before surgery were excluded. LGG was suspected by cMRI when no necrosis or relevant oedema (i.e., absence of oedema or minimal oedema not distinguishable from tumour burden) was observed and when CE was absent or faint [5]. Patients who fulfilled these cMRI criteria underwent all aMRI techniques (PWI, DWI, MRS) and complete cMRI analysis that is routinely performed within the Institute. Clinical and cMRI follow-up was performed every six months.

Magnetic resonance imaging

MRI was performed with a 1.5 T unit (Siemens, Avanto).

cMRI protocol

Sagittal and bi-commissural T1, bi-commissural T2-proton density weighted images (w.i.), coronal Fluid Attenuated Inversion Recovery (FLAIR). Post-contrast volumetric T1 w.i. was performed after PWI. The following features were considered for complete cMRI analysis: homogeneity on T1/T2, presence of CE, mass effect, multifocality, leptomeningeal/subependymal seeding, contralateral. Details in Online Resource 1.

PWI

Dynamic susceptibility-weighted contrast-enhanced (DSC) PWI (Gadovist®, 0.1 cc/Kg, 5 ml/sec and fixed 3 cc prebolus. Maximum tumour cerebral blood volume (CBV) was obtained by identifying regions of maximum perfusion from colour maps. Three regions of interest (ROI) were placed on the highest colour areas of tumours. CBV values were normalized (rCBV) with an identical ROI positioned on the contralateral healthy white matter (CHWM). rCBVmax was obtained from the highest average value ROI.

DWI

Bi-commissural, single-shot echo-planar sequence, 3 orthogonal directions, b values 0–500–1000 s/mm^2. Three ROIs were placed on different areas of the tumour on the basis of cMRI and ADC map appearance. ADC values were normalized (rADC) by those obtained from the CHWM.

MRS

Multivoxel, 2D Proton MRS, point resolved spectroscopic imaging (PRESS) (TR = 1200, TE = 135) fully enclosing the volume of interest. The following features were considered: NAA reduction, choline increase, Cho/Cr (Choline/Creatine) ratio, presence of lactate/lipids. The two highest Cho/Cr were considered for statistical analysis.

Details in Online Resource 2.

Imaging evaluation and histopathological diagnosis

Two experienced neuroradiologists independently reviewed pre-surgical cMRI and aMRI, separately evaluating each advanced technique in light of cMRI and providing tumour grade estimation (LGG vs HGG). In particular, the following parameters were considered suggestive of HGG: rCBV $\geq$1.5 (mean between literature cut-off values [4, 36]), Cho/Cr $\geq$2 [37], rADC <1 [3]. Furthermore, signal heterogeneity of T2/FLAIR, ADC and CBV maps within the whole tumour was taken into account. If consensus wasn't reached, a third neuroradiologist reviewed the case.

Progression was initially assessed according to Macdonald [38]; after RANO criteria publication [39], all cases were re-evaluated accordingly.

Histopathological diagnosis was performed according to the WHO classification of brain tumours [40].

Statistical analysis

Means and standard deviations (sd) were calculated for continuous variables.

Descriptive statistics were obtained using Mann–Whitney U and X^2 tests for continuous and dichotomous variables, respectively.

Sensitivity, specificity, negative and positive predictive values were calculated for cMRI and aMRI using histopathology as a reference standard. Ninety-five percent confidence intervals (95 % CI) were calculated according to the exact method (based on binomial distribution).

Inter-rater reliability between the two radiologists was determined by Cohen's kappa coefficient.

Receiver Operating Characteristic (ROC) curves were estimated to determine rCBV, rADC, Cho/Cr values that achieve optimal sensitivity and specificity for differentiating: (i) LGG versus HGG; (ii) patients with progression versus progression-free patients; (iii) living patients versus dead patients.

PFS and OS were calculated from histopathological diagnosis until disease progression or death/last follow-up if censored. Kaplan–Meier analysis estimated PFS/OS. The log rank test assessed differences in PFS/OS among patients with various radiological or clinical parameters.

SPSS 22.0 for IBM (SPSS Inc., Chicago, IL, USA) was used for statistical analyses.

Results

Validation of criteria of suspected LGG based on cMRI

One-hundred-ninety-six patients were considered for inclusion. Mean interval between radiological examination and subsequent surgery was 18.6 days (range 0–45 days). A total of 89 patients (45.4 %) met the previously mentioned cMRI criteria for LGG (see "Patients"). Thirty (33.8 %) of the 89 suspected LGG were histologically diagnosed as HGG and 57 (64 %) as LGG. In one case histopathology was inconclusive because of inadequate specimen; one tumour was diagnosed as dysembryoplastic neuroepithelial tumour and excluded. Sensitivity of cMRI criteria for differentiation between LGG and HGG was 81.7 % (95 % CI 69.1–90.9) and specificity 100 %. Tumours not fulfilling cMRI criteria for suspected LGG were never histologically diagnosed as LGG. Fourteen (46.6 %) of the 30 tumours diagnosed as HGG at histopathology showed no CE at cMRI, whereas 12 (21.1 %) of the 57 tumours histologically diagnosed as LGG had faint CE.

Sixty-eight of the 89 tumours that met cMRI criteria for LGG were subjected to complete cMRI analysis and PWI, DWI, MRS. They also underwent subsequent statistical analysis, as described in the next paragraphs. The characteristics of these 68 patients (38 males; mean age 39.6 $\pm$ 12.6 years) are reported in Table 1.

Gross total resection was performed in 27 patients, partial resection in 41.

Conventional and advanced MRI

Of 42 histologically diagnosed LGG cases, 78.5 % were identified by complete cMRI analysis and 85.7 % by aMRI (69 % by PWI, 90.5 % by DWI, 64 % by MRS alone).

Of 26 histologically diagnosed HGG cases, 38.4 % were identified by complete cMRI analysis and 53.8 % by aMRI (53.8 % by PWI, 46.1 % by DWI, 57.7 % by MRS alone).

Diagnostic accuracy of cMRI and aMRI relative to pathology is shown in Table 2.

Diagnostic concordance rate of two blinded neuroradiologists in grading of HGG versus LGG was 95 % (inter-rater agreement K = 0.94).

Mean rCBV values were higher in HGG than in LGG ($p = 0.01$). Statistical analysis showed significant differences between grade II/III and IV gliomas ($p = 0.005$ and $p = 0.003$, respectively), not between grade II and III.

Mean rADC values were higher in LGG than in HGG. Statistical significance was reached when grade II/III and IV gliomas were compared ($p = 0.008$ and $p = 0.05$, respectively).

Cho/Cr ratios were similar in grade II and III gliomas and slightly higher in grade IV and in the nodular portions of grade I gliomas. NAA was decreased but present in all lesions. Lactate was detected in one of two grade I lesions, in five (12.5 %) grade II, in one (14.2 %) GBM, whereas lipids were found in two (10.5 %) grade III gliomas. Mean rCBV, rADC, Cho/Cr values are shown in Table 3.

Table 1 Clinical and radiological features of the 68 patients included in the study who met the cMRI criteria for suspected LGG

Histopathological diagnosis	N°	CE	Radiological PD
Low-grade gliomas (LGG)	42	8 (19 %)	28 (67 %)
Grade I	2	2 (100 %)	–
Pylocitic astrocytoma	2	2	–
Grade II	40	6 (15 %)	28 (70 %)
Oligoastrocytoma	22	3	17
Fibrillar astrocytoma	9	1	6
Oligodendroglioma	5	1	2
Not otherwise specified astrocytoma	4	1	3
High-grade Gliomas (HGG)	26	12 (46 %)	19 (73 %)
Grade III	19	6 (32 %)	14 (74 %)
Anaplastic astrocytoma	7	1	7
Anaplastic oligoastrocytoma	12	5	7
Grade IV	7	6 (86 %)	5 (71 %)
Glioblastoma	7	6	5

Radiological progression of disease (PD) was evaluated by cMRI according to the RANO criteria

Table 2 Diagnostic accuracy of cMRI and aMRI related to histopathological diagnosis in 68 patients meeting the cMRI criteria for suspected LGG

	cMRI	PWI	DWI	MRS	aMRI[a]
Sensitivity (%)	78.5	69.0	90.5	64.3	85.7
(95 % CI)	(65.9–91.4)	(50.4–80.4)	(74.4–96.0)	(45.6–76.4)	(68.3–93.0)
Specificity (%)	38.5	53.8	46.2	57.7	53.8
(95 % CI)	(25.7–60.2)	(37.5–72.0)	(25.6–70.4)	(35.0–79.2)	(31.8–76.3)
PPV (%)	67.3	70.7	73.1	71.1	75.0
(95 % CI)	(38.4–83.7)	(56.1–85.4)	(62.0–88.4)	(54.8–85.8)	(64.7–87.4)
PNV (%)	47.6	51.9	75.0	50.0	70.0
(95 % CI)	(25.8–68.5)	(30.9–74.3)	(53.4–87.7)	(32.4–71.2)	(44.8–85.7)

PPV positive predictive value, *NPV* negative predictive value

[a] Comprehensive evaluation of all three aMRI techniques. True positives are cases in which LGG was suspected by radiology and confirmed by histopathology

Because LGG are a non-homogeneous group of tumours arising from astrocytic/oligodendroglial lineages, we compared aMRI data of the most representative LGG types (i.e., fibrillary astrocytoma (FA), oligodendroglioma (ODG), oligoastrocytoma (OA)). ODG had the highest rCBV ($p = 0.04$) and Cho/Cr ($p = 0.05$) and the lowest rADC values (not statistically significant). FA had the lowest rCBV and Cho/Cr and the highest rADC values. Intermediate values were found in OA (Online Resource 3).

Both cMRI and aMRI were able to diagnose pilocytic astrocytomas. All GBM but one were identified as HGG by aMRI. All grade II ODGs but one were correctly diagnosed using aMRI. cMRI and aMRI recognized 26.3 % and 42.8 % of grade III gliomas, respectively (Fig. 1).

rCBV, rADC, rCho/Cr values of optimal sensitivity and specificity in differentiating between LGG and HGG were: 1.29 (sensitivity 61.5 %, specificity 54.7 %), 1.69 (sensitivity 53.8 %, specificity 43 %), 2.1 (sensitivity 53.8 %, specificity 64.3 %), respectively.

Clinical-radiological outcome

During follow-up (median 60 months, range 4–84), 47 of the 68 LGG patients showed radiological progression according to RANO [24] (Table 1). The patients histologically diagnosed with HGG were treated with radiochemotherapy (temozolomide) after surgery, whereas LGG patients received radiotherapy and/or chemotherapy at progression. Twenty-five patients died due to progression, three for other reasons (melanoma, suicide, unknown cause).

Median PFS and OS of all patients were 51 and 80 months, respectively. PFS at 6, 12, 36 months was 95, 92, 75 % for LGG patients and 88, 61, 45 %, for HGG patients, respectively (not significant). OS at 12, 36,

Table 3 Mean values of aMRI parameters: PWI (rCBV), DWI (rADC), and MRS (Cho/Cr)

	Low-grade gliomas (n = 42)			High-grade gliomas (n = 26)		
	LGG	Grade I (n = 2)	Grade II (n = 40)	HGG	Grade III (n = 19)	Grade IV (n = 7)
rCBV						
Max ± SD	1.6 ± 1.5	1.9 ± 1.2	1.6 ± 1.5	2.1 ± 1.6	1.6 ± 0.9	3.6 ± 2.1
Mean ± SD	1.2 ± 0.9	1.1 ± 0.4	1.2 ± 1.0	1.8 ± 1.4	1.3 ± 0.8	2.8 ± 2.0
rADC						
Min ± SD	1.8 ± 0.4	2.0 ± 0.4	1.8 ± 0.4	1.5 ± 0.7	1.7 ± 0.7	1.2 ± 0.6
Mean ± SD	2.1 ± 0.4	2.7 ± 0.7	2.0 ± 0.4	1.7 ± 0.6	1.8 ± 0.6	1.4 ± 0.6
Cho/Cr						
Max ± SD	1.9 ± 0.6	2.5 ± 0.7	1.8 ± 0.6	2.0 ± 0.6	2.0 ± 0.6	2.2 ± 0.8
Mean ± SD	1.7 ± 0.4	1.9 ± 0.1	1.7 ± 0.5	1.9 ± 0.6	1.8 ± 0.6	2.1 ± 0.8

60 months was 92, 65, 53 % for HGG patients and 97, 88, 80 %, for LGG patients, respectively ($p = 0.01$).

Maximum rCBV, minimum rADC, maximum rCho/Cr values that achieved optimal sensitivity and specificity for survival correlations were 1.46 (sensitivity 50 %, specificity 59.9 %), 1.69 (sensitivity 72 %, specificity 72 %), and 2 (sensitivity 55.8 %, specificity 56 %), respectively.

Significantly longer OS was observed in patients with maximum rCBV <1.46 and minimum rADC >1.69 (80 vs 55 months, $p = 0.01$; 80 vs 51 months, $p = 0.002$, respectively, Fig 2). This result was also confirmed when cases were stratified according to pathology (LGG vs HGG. Figure 2) and presence/absence of CE in cMRI. A trend of longer PFS was observed for rCBV <1.46 and rADC >1.69.

Furthermore, the ability of aMRI to predict OS increased when an increasing number of aMRI techniques were considered. Longer OS was observed in patients with no abnormal parameters compared to patients with one or with two-or-more abnormal parameters: eighty-month survival was achieved by patients without abnormal parameters, *not reached* in patients with one abnormal parameter, 55-month in the others ($p = 0.033$). This was also confirmed when cases were stratified according to pathology (LGG vs HGG, $p = 0.04$).

No significant association between age, gender, presence of CE at cMRI and prognosis was recorded.

For survival of patients with mismatched radiologic versus histopathological diagnoses, see Online Resource 4.

Discussion

In a cohort of patients with suspected supratentorial glioma on cMRI who were candidates for surgery, a group of 68 that satisfied all three cMRI criteria for LGG (no necrosis, no relevant oedema, absent or faint CE) was subjected to aMRI. Compared to histology, cMRI underestimated the fraction of HGG. Sensitivity of cMRI in differentiating HGG from LGG, which ranges 55–83 % in the literature [3, 4], reached 78.5 % in the present study. aMRI increased sensitivity to 85.7 %, but specificity was 53.8 %, indicating that aMRI just slightly increases diagnostic accuracy compared to histopathology.

Interestingly, 37.5 % of gliomas that were suggested to be high grade by one aMRI technique were histologically diagnosed as HGG. This percentage increased to 61.5 % with two techniques (in accordance with previous multiparametric analysis [4, 41, 42]) and to 66.7 % with three techniques.

Anaplastic gliomas may mimic the appearance of LGG, lacking CE and having minimal oedema. The tumours in our population of radiologically suspected LGG that were histologically diagnosed as HGG were non-enhancing or faintly enhancing with no oedema and no necrosis. All histological GBM that were suspected of being LGG had MRI features of secondary GBM, lacking ring CE and cystic-necrotic areas [43]. ROI positioning (especially in partially resected LGG) might explain discrepancies with histopathology.

Though tumour-growth-rate was correlated with survival in LGG [44], as long as stratification of LGG is based on morphology, the clinical management of these tumours often remains challenging. Currently, important decisions impacting patient therapy should be supported by complementary technologies, such as aMRI and molecular [45] analysis to improve neuropathological diagnosis.

Previously published studies showed differences in aMRI parameters for LGG versus HGG: rCBV [4, 9, 10, 28, 46] and Cho/Cr [4, 12, 36, 47] were higher in HGG and rADC was lower [3, 9, 11, 13, 14].

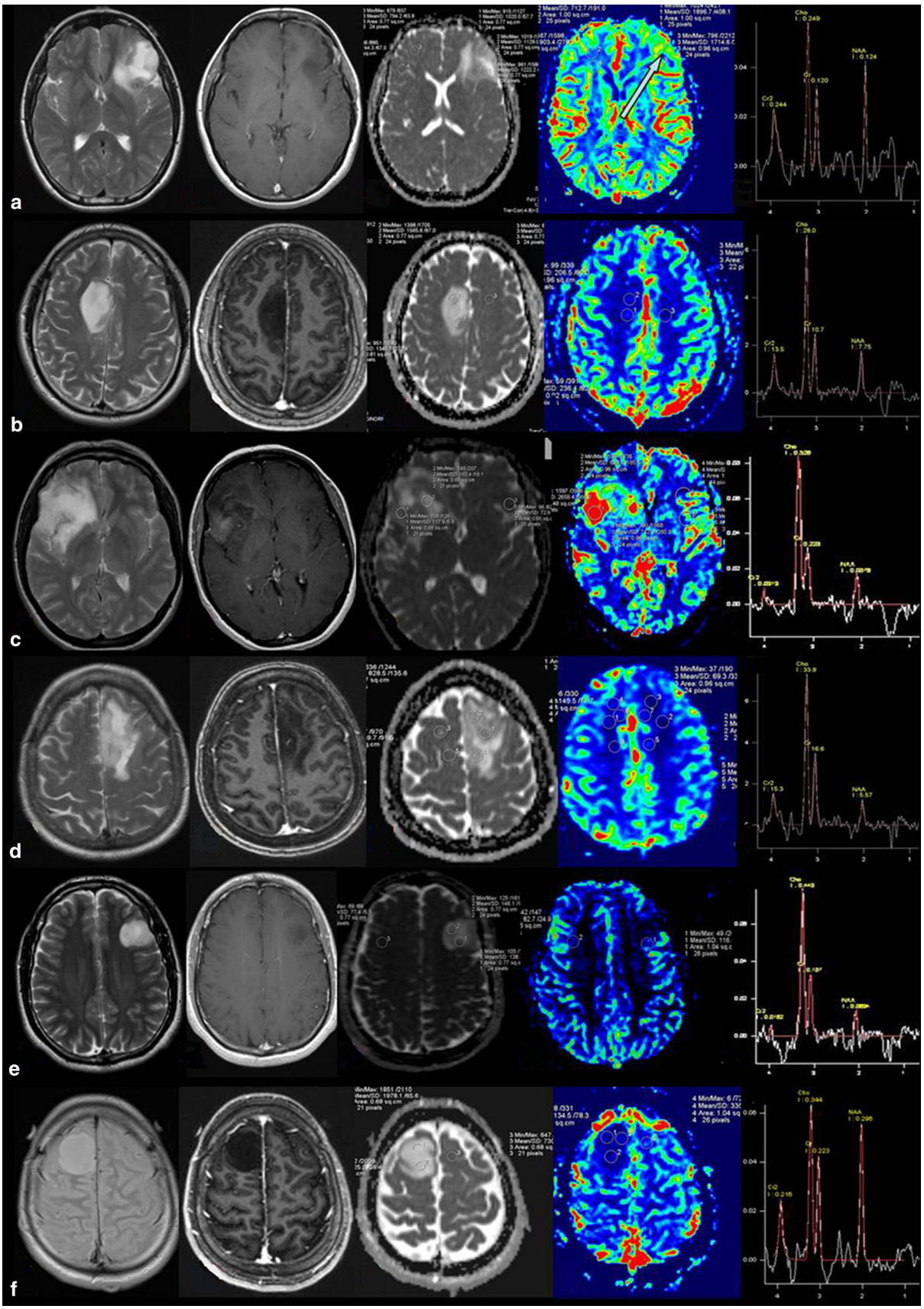
a
b
c
d
e
f

◀**Fig. 1** Examples of cMRI and aMRI glioma assessment. In *each row*, from *left* to *right*, T2 and T1 images with contrast agent, ADC, CBV and MRS are shown, respectively. **a** Glioblastoma. cMRI suggests LGG. Low ADC and high rCBV were most pronounced in the antero-lateral portion of the tumour in a ring-like shape (*arrow* in the *fourth panel*). High Cho/Cr and lactate *peaks* indicate HGG. The PFS and OS were 8 and 26 months, respectively. **b** Glioblastoma. cMRI with high ADC and low rCBV that suggests LGG; only the high Cho/Cr indicates HGG. The PFS and OS were 33 and >49 months, respectively, and the patient in currently alive. **c** Oligodendroglioma. From *left to right* dubious HGG by cMRI due to heterogeneously and poorly defined signal intensity on T2 w.i. and faint CE. Low rADC in many regions of the tumour, very high homogeneous rCBV, and high Cho/Cr are typical findings of oligodendrogliomas. Both the PFS and OS were >84 months, and the patient is currently free from disease. **d** Oligodendroglioma. Heterogeneous abnormal signal intensity on T2-weighted images of cMRI without CE and with low rADC, low rCBV and high Cho/Cr. The atypical finding of this oligodendroglioma is low rCBV. The PFS and OS were 33 and >65 months, respectively, and the patient is currently alive. **e** Anaplastic astrocytoma. cMRI showing a well-defined and homogenous lesion without CE and with low rCBV that suggests LGG. Low ADC and high Cho/Cr and lactate peaks indicate HGG. The PFS and OS were 43 and 80 months, respectively. **f** Anaplastic astrocytoma. cMRI and aMRI suggest LGG. Both the PFS and OS were >57 months, and the patient is currently free from disease

A few authors set different cut-off values between LGG and HGG, ranging 0.94–3.34 [4, 11, 21, 36, 41, 42] for rCBV, 0.31–1.31 [3, 22–24, 36, 42, 48] for rADC, 1.3–2.04 [4, 20, 25, 26, 37, 42] for Cho/Cr. These thresholds were obtained mainly in populations that included a majority of GBM and few LGG patients, and overlapping values were observed within grade II and III lesions. In the largest cohort of unselected gliomas (120 HGG, 40 LGG), Law [4] identified a threshold 1.75 for rCBV and 1.56 for Cho/Cr. A cut-off of 1.07 for DWI was found in another group of 74 gliomas (37 GBM, 22 anaplastic astrocytomas, 15 LGG) [22].

In our population, cut-off values for HGG versus LGG were 1.29 for rCBV and 1.69 for rADC. The best cut-off value for Cho/Cr was 2.1, ensuring both sensitivity and specificity higher than 50 %.

PWI was considered predictive of tumour grade in previous studies because it shows diverse rCBV values in LGG, HGG [4, 9, 10, 36] and ODG [13]. In our cohort, the differences in rCBV significantly distinguished LGG from HGG and GBM from grade II-III gliomas, but not grade II from grade III gliomas. Mean rCBV values in our HGG patients were lower than those previously reported, which is probably due to patient selection, while rCBV in our LGG patients were similar to literature [9, 25].

In our cohort, DWI showed lower rADC in HGG than in LGG due to increased cellularity, one of the earliest features of anaplastic progression [12]. Lower ADC and higher CBV in HGG than in LGG patients were previously detected by Fan in 22 non-enhancing gliomas [9] and by Murakami and Khalid, who also published ADC cut-off values to distinguish grade II from grade III gliomas [23, 24]. In contrast, other authors [29, 48, 49] didn't find significant differences in ADC values when comparing grade II versus III gliomas, which is consistent with our results. For more details, see Online Resource 5.

In our MRS analysis, we found that Cho/Cr ratio improved diagnostic accuracy compared to cMRI. Values were similar in grades I to III and slightly higher in grade IV, so that the cut-off value that optimally stratified LGG and HGG wasn't statistically significant [41, 47]. However, previous studies reported that MRS is able to detect initial shifts to anaplasia sooner than other MRI techniques [20], identifying choline level as a useful parameter in determining glioma grade [4, 25, 26, 37, 42].

In agreement with the literature [14, 32, 50], our cohort of ODG had rCBV and Cho/Cr values higher than those of other LGG and similar to those of GBM because of high neovascularization and vessel hyperplasia [43]. OA appeared more heterogeneous, and recent developments in molecular genetics have cast doubt on its relevance as a distinct entity [45].

Apart from their use in stratification of LGG and in distinguishing LGG from HGG, radiological markers can be useful for survival prediction. A few recent studies correlated PWI, DWI and MRS measurements with time to progression or death [10, 31] and suggested cut-off values to distinguish early progressive from less aggressive, histologically diagnosed LGG [20, 25, 27, 29, 31–35] (Online Resource 6). However, many of these publications were limited to small cohorts of LGG or had short follow-up; moreover, their analysis mainly focused on CBV values and on PFS as an outcome parameter. A rCBV threshold of 1.75 was described to discriminate long from short survival in grade II gliomas [27, 31, 33]. Furthermore, a meta-analysis aimed at determining whether ADC values predict prognosis confirmed the predictive value of ADC on survival in HGG independently of histopathological grade [30].

In an outcome-based analysis, our rCBV and rADC cut-off values were able to stratify tumours, leading to different OS. Patients with radiological progression and shorter OS had lower rADC and higher rCBV values when compared to subjects with longer survival. In addition to predicting histological grade, aMRI was able to predict survival with an accuracy that improved as the number of aMRI parameters that meet the identified cutoffs increased, as significantly longer OS was observed in patients with no abnormal parameters compared to patients with one or two-or-more abnormal parameters. This trend is relatively independent of histological grade, which is in agreement with recent data that defines lower-grade gliomas [45].

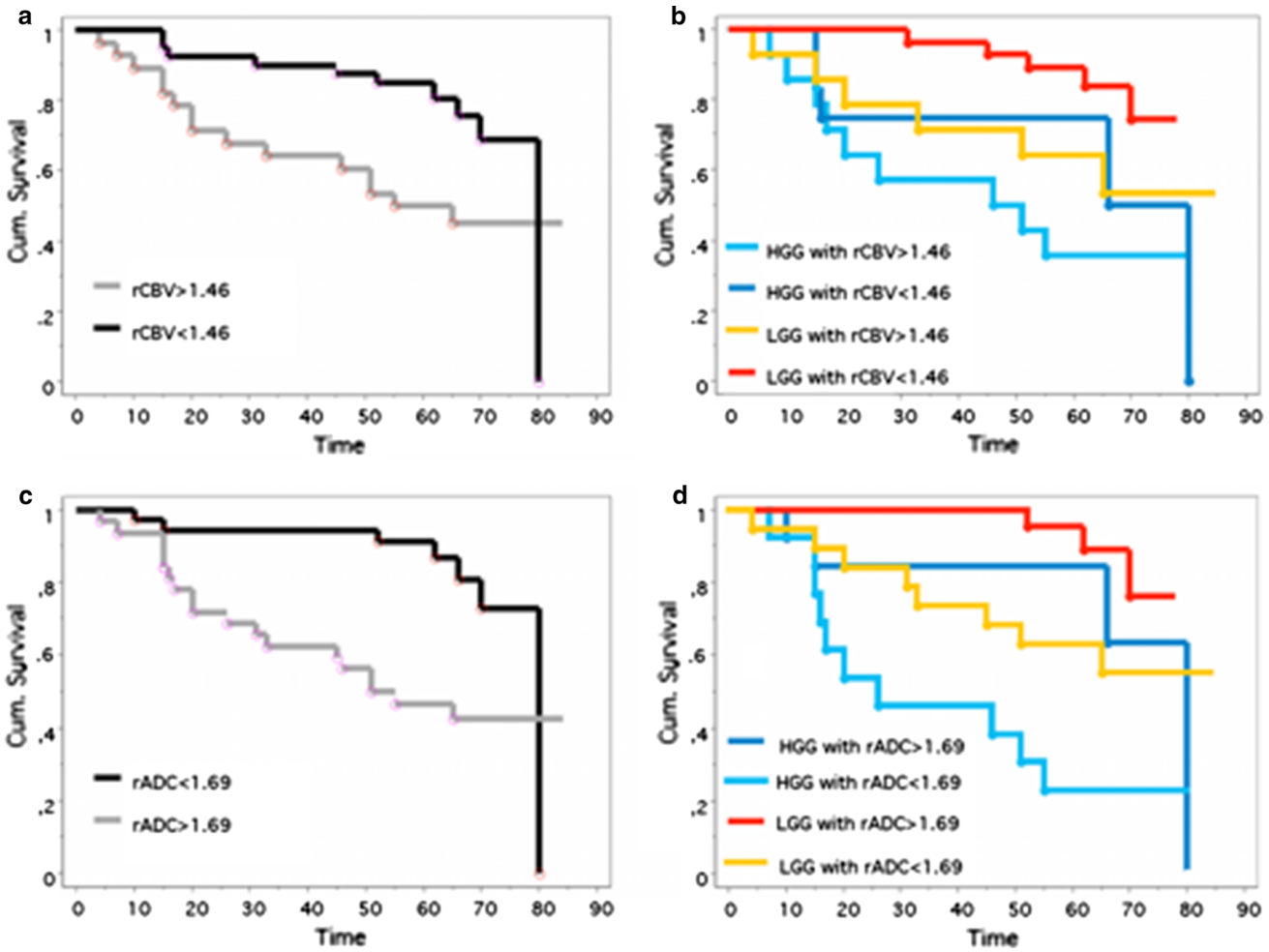

Fig. 2 Kaplan–Meier curves showing the OS of the cohort of 68 patients when rADC (**a** and **b**) and rCBV (**c** and **d**) cut-off values are 1.69 and 1.46, respectively. **b** and **d** show results after stratification by tumour grade

In conclusion, our results suggest that aMRI slightly improves the accuracy of cMRI in distinguishing LGG from HGG; in particular, aMRI allowed the detection of malignant features in GBM that appear as LGG on cMRI and confirmed specific characteristics of ODG helping their differentiation from other gliomas. Notably, DWI and PWI can be of value in predicting OS in lower-grade gliomas independent of their grading. These observations support the integration of imaging with pathology and genetics to provide more robust classification of lower-grade gliomas and strengthen the rationale for treatment decisions.

Acknowledgments This work was supported by funding from the Associazione Italiana per la Ricerca sul Cancro (AIRC) to G. Filippini and from the Italian Ministry of Health to G. Finocchiaro. We wish to thank Valter Torri and Greta Brenna for their statistical support.

Compliance with ethical standards

Conflict of interest The authors declare that they have no conflict of interest.

Ethical standards All procedures performed in this study involving human participants were in accordance with the ethical standards of the institutional research committee and with the 1964 Helsinki declaration and its later amendments or comparable ethical standards.

Informed consent Informed consent was obtained from all individual participants included in the study.

References

1. Ruiz J, Lesser GJ (2009) Low-grade gliomas. Curr Treat Options Oncol 10:231–242
2. Lang FF, Gilbert MR (2006) Diffusely infiltrative low-grade gliomas in adults. J Clin Oncol 24:1236–1245
3. Bulakbasi N, Guvenc I, Onguru O, Erdogan E, Tayfun C, Ucoz T (2004) The added value of the apparent diffusion coefficient calculation to magnetic resonance imaging in the differentiation and grading of malignant brain tumors. J Comput Assist Tomogr 28:735–746
4. Law M, Yang S, Wang H, Babb JS, Johnson G, Cha S, Knopp EA, Zagzag D (2003) Glioma grading: sensitivity, specificity, and

predictive values of perfusion MR imaging and proton MR spectroscopic imaging compared with conventional MR imaging. AJNR Am J Neuroradiol 24:1989–1998
5. Pallud J, Capelle L, Taillandier L et al (2009) Prognostic significance of imaging contrast enhancement for WHO grade II gliomas. Neuro Oncol 11:176–182
6. Scarabino T, Popolizio T, Trojsi F, Giannatempo G, Pollice S, Maggialetti N, Carriero A, Di Costanzo A, Tedeschi G, Salvolini U (2009) Role of advanced MR imaging modalities in diagnosing cerebral gliomas. Radiol Med 114:448–460
7. Kim JH, Chang KH, Na DG, Song IC, Kwon BJ, Han MH, Kim K (2006) 3T 1H-MR spectroscopy in grading of cerebral gliomas: comparison of short and intermediate echo time sequences. Am J Neuroradiol 27:1412–1418
8. Weber M-A, Giesel FL, Stieltjes B (2008) MRI for identification of progression in brain tumors: from morphology to function. Expert Rev Neurother 8:1507–1525
9. Fan GG, Deng QL, Wu ZH, Guo QY (2006) Usefulness of diffusion/perfusion-weighted MRI in patients with non-enhancing supratentorial brain gliomas: a valuable tool to predict tumour grading? Br J Radiol 79:652–658
10. Chaskis C, Stadnik T, Michotte A, Van Rompaey K, D'Haens J (2006) Prognostic value of perfusion-weighted imaging in brain glioma: a prospective study. Acta Neurochir (Wien) 148:277–285
11. Arvinda HR, Kesavadas C, Sarma PS, Thomas B, Radhakrishnan VV, Gupta AK, Kapilamoorthy TR, Nair S (2009) Glioma grading: sensitivity, specificity, positive and negative predictive values of diffusion and perfusion imaging. J Neurooncol 94:87–96
12. McKnight TR, Lamborn KR, Love TD, Berger MS, Chang S, Dillon WP, Bollen A, Nelson SJ (2007) Correlation of magnetic resonance spectroscopic and growth characteristics within Grades II and III gliomas. J Neurosurg 106:660–666
13. Chang SM, Nelson S, Vandenberg S et al (2009) Integration of preoperative anatomic and metabolic physiologic imaging of newly diagnosed glioma. J Neurooncol 92:401–415
14. Sugahara T, Korogi Y, Kochi M et al (1999) Usefulness of diffusion-weighted MRI with echo-planar technique in the evaluation of cellularity in gliomas. J Magn Reson Imaging 9:53–60
15. Gerstner ER, Sorensen AG, Jain RK, Batchelor TT (2008) Advances in neuroimaging techniques for the evaluation of tumor growth, vascular permeability, and angiogenesis in gliomas. Curr Opin Neurol 21:728–735
16. Weber MA, Zoubaa S, Schlieter M et al (2006) Diagnostic performance of spectroscopic and perfusion MRI for distinction of brain tumors. Neurology 66:1899–1906
17. Xu V, Chan H, Lin AP, Sailasuta N, Valencerina S, Tran T, Hovener J, Ross BD (2008) MR spectroscopy in diagnosis and neurological decision-making. Semin Neurol 28:407–422
18. Lam WWM, Poon WS, Metreweli C (2002) Diffusion MR imaging in glioma: does it have any role in the pre-operation determination of grading of glioma? Clin Radiol 57:219–225
19. Al-Okaili RN, Krejza J, Wang S, Woo JH, Melhem ER (2006) Advanced MR imaging techniques in the diagnosis of intraaxial brain tumors in adults. Radiographics 26(Suppl 1):S173–S189
20. Hlaihel C, Guilloton L, Guyotat J, Streichenberger N, Honnorat J, Cotton F (2010) Predictive value of multimodality MRI using conventional, perfusion, and spectroscopy MR in anaplastic transformation of low-grade oligodendrogliomas. J Neurooncol 97:73–80
21. Morita N, Wang S, Chawla S, Poptani H, Melhem ER (2010) Dynamic susceptibility contrast perfusion weighted imaging in grading of nonenhancing astrocytomas. J Magn Reson Imaging 32:803–808
22. Server A, Kulle B, Gadmar ØB, Josefsen R, Kumar T, Nakstad PH (2011) Measurements of diagnostic examination performance using quantitative apparent diffusion coefficient and proton MR spectroscopic imaging in the preoperative evaluation of tumor grade in cerebral gliomas. Eur J Radiol 80:462–470
23. Murakami R, Hirai T, Sugahara T et al (2009) Grading astrocytic tumors by using apparent diffusion coefficient parameters: superiority of a one- versus two-parameter pilot method. Radiology 251:838–845
24. Khalid L, Carone M, Dumrongpisutikul N, Intrapiromkul J, Bonekamp D, Barker PB, Yousem DM (2012) Imaging characteristics of oligodendrogliomas that predict grade. Am J Neuroradiol 33:852–857
25. Sahin N, Melhem ER, Wang S, Krejza J, Poptani H, Chawla S, Verma G (2013) Advanced MR imaging techniques in the evaluation of nonenhancing gliomas: perfusion-weighted imaging compared with proton magnetic resonance spectroscopy and tumor grade. Neuroradiol J 26:531–541
26. Liu Z, Zhou Q, Zeng Q, Li C-F, Zhang K (2012) Noninvasive evaluation of cerebral glioma grade by using diffusion-weighted imaging-guided single-voxel proton magnetic resonance spectroscopy. J Int Med Res 40:76–84
27. Law M, Young RJ, Babb JS, Peccerelli N, Chheang S, Gruber ML, Miller DC, Golfinos JG (2008) Gliomas: predicting time to progression or survival with cerebral blood volume measurements at dynamic susceptibility-weighted contrast-enhanced perfusion MR imaging. Radiology 2:490–498
28. Maia ACM, Malheiros SMF, da Rocha AJ, da Silva CJ, Gabbai AA, Ferraz FAP, Stávale JN (2005) MR cerebral blood volume maps correlated with vascular endothelial growth factor expression and tumor grade in nonenhancing gliomas. AJNR Am J Neuroradiol 26:777–783
29. Cui Y, Ma L, Chen X, Zhang Z, Jiang H, Lin S (2014) Lower apparent diffusion coefficients indicate distinct prognosis in low-grade and high-grade glioma. J Neurooncol 119:377–385
30. Zulfiqar M, Yousem DM, Lai H (2013) ADC values and prognosis of malignant astrocytomas: does lower ADC predict a worse prognosis independent of grade of tumor?-a meta-analysis. Am J Roentgenol 200:624–629
31. Caseiras GB, Chheang S, Babb J et al (2010) Relative cerebral blood volume measurements of low-grade gliomas predict patient outcome in a multi-institution setting. Eur J Radiol 73:215–220
32. Bisdas S, Kirkpatrick M, Giglio P, Welsh C, Spampinato MV, Rumboldt Z (2009) Cerebral blood volume measurements by perfusion-weighted MR imaging in gliomas: ready for prime time in predicting short-term outcome and recurrent disease? Am J Neuroradiol 30:681–688
33. Majchrzak K, Kaspera W, Bobek-Billewicz B, Hebda A, Stasik-Pres G, Majchrzak H, Ladzinski P (2012) The assessment of prognostic factors in surgical treatment of low-grade gliomas: a prospective study. Clin Neurol Neurosurg 114:1135–1144
34. Hattingen E, Delic O, Franz K, Pilatus U, Raab P, Lanfermann H, Gerlach R (2010) (1)H MRSI and progression-free survival in patients with WHO grades II and III gliomas. Neurol Res 32:593–602
35. Lober RM, Cho YJ, Tang Y, Barnes PD, Edwards MS, Vogel H, Fisher PG, Monje M, Yeom KW (2014) Diffusion-weighted MRI derived apparent diffusion coefficient identifies prognostically distinct subgroups of pediatric diffuse intrinsic pontine glioma. J. Neurooncol. 117:175–182
36. Zonari P, Baraldi P, Crisi G (2007) Multimodal MRI in the characterization of glial neoplasms: the combined role of single-voxel MR spectroscopy, diffusion imaging and echo-planar perfusion imaging. Neuroradiology 49:795–803
37. Senft C, Hattingen E, Pilatus U, Franz K, Schänzer A, Lanfermann H, Seifert V, Gasser T (2009) Diagnostic value of proton magnetic resonance spectroscopy in the noninvasive grading of solid gliomas: comparison of maximum and mean choline values. Neurosurgery 65:908–913

38. Macdonald DR, Cascino TL, Schold SC Jr, Cairncross JG (1990) Response criteria for phase II studies of supratentorial malignant glioma. J Clin Oncol 8:1277–1280
39. Van den Bent MJ, Wefel JS, Schiff D et al (2011) Response assessment in neuro-oncology (a report of the RANO group): assessment of outcome in trials of diffuse low-grade gliomas. Lancet Oncol 12:583–593
40. Louis DN, Ohgaki H, Wiestler OD, Cavenee WK, Burger PC, Jouvet A, Scheithauer BW, Kleihues P (2007) The 2007 WHO classification of tumours of the central nervous system. Acta Neuropathol 114:97–109
41. Roy B, Gupta RK, Maudsley AA et al (2013) Utility of multiparametric 3-T MRI for glioma characterization. Neuroradiology 55:603–613
42. Yoon JH, Kim JH, Kang WJ, Sohn C-HH, Choi SH, Yun TJ, Eun Y, Song YS, Chang K-HH (2014) Grading of cerebral glioma with multiparametric MR imaging and 18F-FDG-PET: concordance and accuracy. Eur Radiol 24:380–389
43. Eoli M, Menghi F, Bruzzone MG et al (2007) Methylation of O6-methylguanine DNA methyltransferase and loss of heterozygosity on 19q and/or 17p are overlapping features of secondary glioblastomas with prolonged survival. Clin Cancer Res 13:2606–2613
44. Pallud J, Blonski M, Mandonnet E, Audureau E, Fontaine D, Sanai N, Bauchet L, Peruzzi P, Frenay M, Colin P, Guillevin R, Bernier V, Baron MH, Guyotat J, Duffau H, Taillandier L, Capelle L (2013) Velocity of tumor spontaneous expansion predicts long-term outcomes for diffuse low-grade gliomas. Neuro-oncol 15(5):595–606
45. Cancer Genome Atlas Research Network (2015) Comprehensive, integrative genomic analysis of diffuse lower-grade gliomas. NEJM 372(26):2481–2498
46. Haegler K, Wiesmann M, Böhm C, Freiherr J, Schnell O, Brückmann H, Tonn JC, Linn J (2012) New similarity search based glioma grading. Neuroradiology 54:829–837
47. Bradac O, Vrana J, Jiru F, Kramar F, Netuka D, Hrabal P, Horinek D, de Lacy P, Benes V (2014) Recognition of anaplastic foci within low-grade gliomas using MR spectroscopy. Br J Neurosurg 28:631–636
48. Hilario A, Ramos A, Perez-Nuñez A, Salvador E, Millan JM, Lagares A, Sepulveda JM, Gonzalez-Leon P, Hernandez-Lain A, Ricoy JR (2012) The added value of apparent diffusion coefficient to cerebral blood volume in the preoperative grading of diffuse gliomas. Am J Neuroradiol 33:701–707
49. Liu X, Tian W, Kolar B, Yeaney GA, Qiu X, Johnson MD, Ekholm S (2011) MR diffusion tensor and perfusion-weighted imaging in preoperative grading of supratentorial nonenhancing gliomas. Neuro Oncol 13:447–455
50. Cha S, Tihan T, Crawford F, Fischbein NJ, Chang S, Bollen A, Nelson SJ, Prados M, Berger MS, Dillon WP (2005) Differentiation of low-grade oligodendrogliomas from low-grade astrocytomas by using quantitative blood-volume measurements derived from dynamic susceptibility contrast-enhanced MR imaging. Am J Neuroradiol 26:266–273